Unusual static and dynamical characteristics of domain evolution in ferroelectric superlattices

S. Lisenkov,* I. Ponomareva, and L. Bellaiche
Department of Physics, University of Arkansas, Fayetteville, Arkansas 72701, USA
(Received 24 October 2008; published 6 January 2009)

The evolution from nanostripes to monodomains is explored in ferroelectric $BaTiO_3/SrTiO_3$ (BT/ST) superlattices under dc and ac electric fields via the use of a first-principles-based technique. Such evolution involves original states that result in the decoupling of (static and dynamical) properties between BT versus ST layers. For instance, domain walls of nanostripes move at a different speed inside BT versus ST layers, and one intermediate state consists of three-dimensional nanobubbles inside BT layers coexisting with a monodomain inside ST layers. Moreover, velocities of domain walls of nanostripes and nanobubbles are determined as a function of the magnitude and frequency of the applied electric field. The domain-wall motion in BT and ST layers is found to follow a previously determined equation at small fields. On the other hand, velocities of domain walls of nanostripes and nanobubbles are found to obey a different empirical law at higher fields.

DOI: 10.1103/PhysRevB.79.024101 PACS number(s): 77.80.Dj, 68.65.Cd, 77.80.Bh, 77.80.Fm

I. INTRODUCTION

Ferroelectric nanostructures are currently receiving a lot of attention because of their potential in leading toward miniaturized devices[1] and in exhibiting striking new phenomena.[2–4] For instance, stripes of "up" and "down" dipoles with exceptionally small periodicity (on the order of a few nanometers) have been recently discovered in ferroelectric ultrathin films.[5,6] Recent studies further predicted an unusual evolution of such nanostripes when these films are placed under static electric field.[7,8] Similarly, different nanostripe domain structures have also been very recently discovered[9] in another type of ferroelectric nanostructures, namely, superlattices (SLs), which are heterostructures consisting of alternating layers of two or more materials.[10] Superlattices have recently generated a flurry of theoretical and experimental works[3,9–15] but we are not aware of any study devoted to evolution of nanostripes in ferroelectric superlattices under electric fields. It is worth realizing that such latter findings in thin films and superlattices all concern *static* properties. This implies that important *dynamical* information (such as the domain-wall velocity and nanostripe and nanobubble morphology under ac electric fields) are completely unknown in ferroelectric nanostructures despite their obvious fundamental importance and technological relevance (for instance, the motion of domain walls is critical to fast high-density nonvolatile random access memory[16]). One may also wonder if electric fields can decouple static and/or dynamical properties of different kinds of layers in superlattice, which would contrast with the common belief that different layers should behave in a similar fashion due to electrostatic reasons.[17]

Motivated to resolve the issues aforementioned, we used a first-principles-based scheme to investigate the evolution of nanostripe domains in $BaTiO_3/SrTiO_3$ superlattice under both dc *and* ac electric fields (note that such systems are likely the most studied and promising ferroelectric superlattices to date, partly due to the success in growing high-quality samples[10,18]). The aim of this paper is to report (i) original "decoupled" static and dynamical features (such as coexistence of different phases inside $BaTiO_3$ and $SrTiO_3$ layers, or domain walls moving with different speeds in the $BaTiO_3$ and $SrTiO_3$ layers), and (ii) different empirical laws governing the velocity associated with domain-wall motion of stripes and bubbles at high fields. We also discuss the microscopic reasons for such features and laws.

II. METHOD

Here, we consider a $[BaTiO_3]_n/[SrTiO_3]_n$ (BT/ST) superlattice with a period of $n=10$, epitaxially grown on a $SrTiO_3$ substrate, and subject to an electric field, **E**, applied along the SL growth direction (that is, the z axis which is chosen to be along the pseudocubic [001] direction). Such a system is modeled by a $24\times24\times20$ periodic supercell (57 600 atoms). Its total energy is given by the sum of the first-principles-based effective Hamiltonian energy[19] and an additional term representing the coupling with electric field.[20] The epitaxial situations are mimicked by freezing some strain variables so that *each* layer in the superlattice has the in-plane lattice constant of the chosen substrate.[9] The total energy of this effective Hamiltonian is used with a Monte Carlo (MC) technique[21] to simulate dc electric field and with a molecular-dynamics (MD) technique to simulate ac electric field. The latter one is given by $E_0\sin(2\pi\nu t)$, where E_0 and ν are the amplitude and frequency of the field, respectively, while t is the time. In MD simulations, Newton's equations of motion are solved for all the degrees of freedom included in the effective Hamiltonian approach. Note that using the effective Hamiltonian approach of Ref. 19 has been proven to yield static and dynamical properties in good agreement with experiment and direct first-principles data for disordered $Ba_{1-x}Sr_xTiO_3$ systems and BT/ST superlattices.[9,19,22,23] More details about the energetic terms included in this effective Hamiltonian approach and its parameters can be found in Ref. 19.

III. RESULTS

A. dc electric fields

We first investigate the evolution of the nanostripe domain structure in epitaxially strained BT/ST superlattices with relatively large periods[9] under dc electric field at 10 K. As shown in Ref. 9, such structure possesses both 180° periodic nanostripes, for the z component of its dipoles, alter-

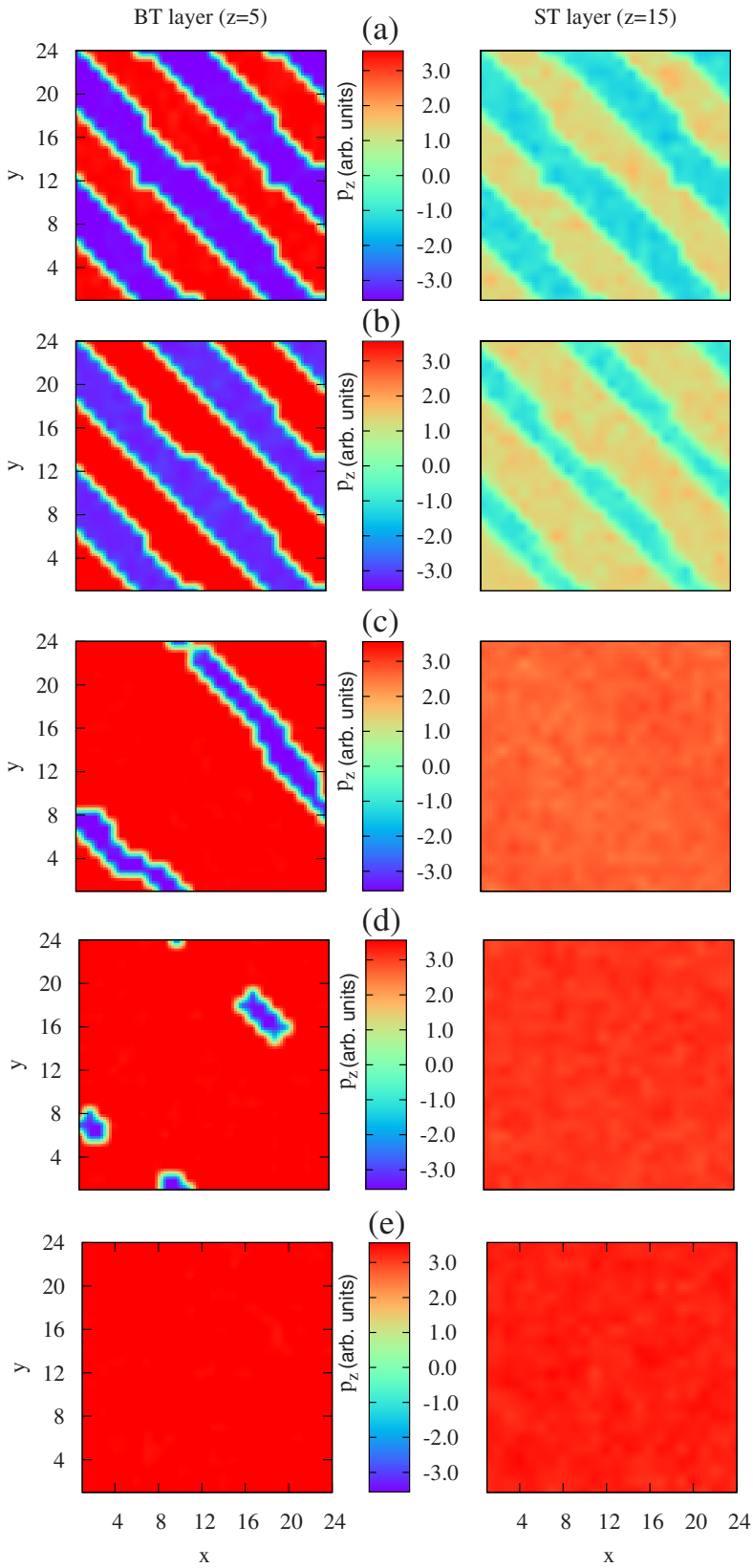

FIG. 1. (Color online) (001) cross sections of dipole patterns in a BT layer (left column) and ST layer (right column), at $T=10$ K, in the $[BaTiO_3]_{10}/[SrTiO_3]_{10}$ SL for different dc electric fields: (a) $E=0.0$ MV/cm (ground state), (b) $E=2.65$ MV/cm (region I), (c) $E=3.0$ MV/cm (region II), (d) $E=4.5$ MV/cm (region III), and (e) $E=5.8$ MV/cm (region IV). The color reflects the out-of-plane (p_z) component of the electric-dipole moment.

nating along the [110] direction in the BT and ST layers with a periodicity of 33 Å [see Fig. 1(a)], and a spontaneous polarization along the $[\bar{1}10]$ direction that originates from the ST layers.[9] The formation of such nanostripes is governed by the different absolute value of the z component of the dipoles in the BT versus ST epitaxial layers. If all the dipoles would have pointed along the (up or down) z direction, a large depolarizing field would thus have existed inside the BT and ST layers. To avoid that, our (long-period) superlattice decides to exhibit domains, as in films under open-circuit-like

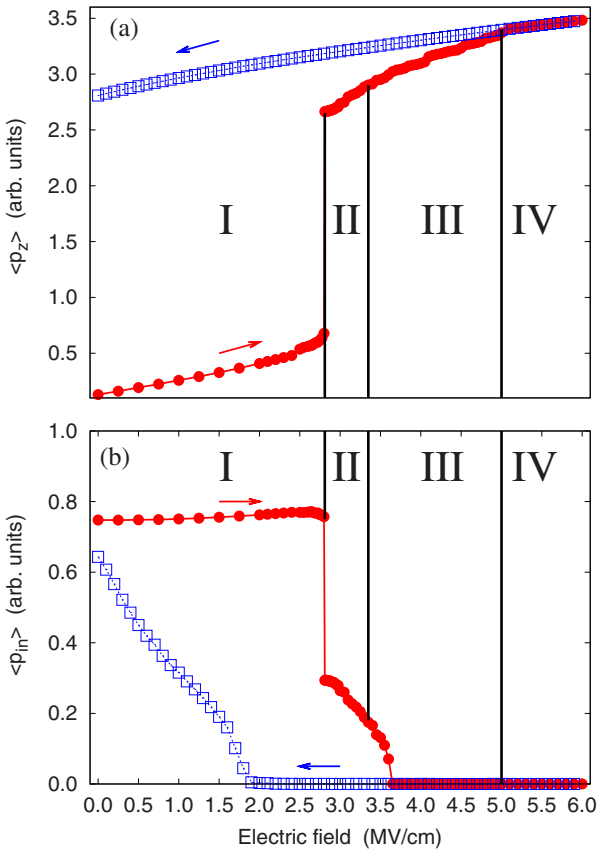

FIG. 2. (Color online) (a) out-of-plane $\langle p_z \rangle$ and (b) in-plane $\langle p_{in} \rangle$ components of the average electric-dipole moment as a function of the magnitude of the dc field at 10 K. The red and blue colors correspond to increasing and decreasing fields, respectively. Regions I–IV are discussed in the text, and correspond to the different dipole configurations found when increasing the field.

conditions.[5–8] (Note that depolarizing field effects are naturally included in our used effective Hamiltonian[9] because this latter technique contains long-range dipolar interactions and because it takes into account the difference in size between Ba and Sr atoms that results in a different magnitude of the dipoles between the BT and ST layers.) Moreover, the fact that there is a spontaneous polarization inside the ST layers can be seen as a precursor effect of the dipoles (inside both ST and BT layers) being all oriented along the $[\bar{1}10]$ direction when the superlattice is under strong enough tensile strain.[9,24]

Under increasing dc field, four different regions (to be denoted as regions I–IV, respectively) can be distinguished. Figures 1(b)–1(e) and Fig. 2 provide atomistic and macroscopic details, respectively, about these regions. For instance, they indicate that most of region I is characterized by the field-induced motions of domain walls in $SrTiO_3$ layers, leading to the shrinking of the down domains and expanding of the up domains (here, down and up refer to directions of the dipoles that are antiparallel and parallel, respectively, to the applied field) while domain walls do *not* move in $BaTiO_3$ layers [see Fig. 1(b)]. The motion of the domain walls in the ST layers results in the increasing of the out-of-plane macroscopic dipole moment while the in-plane dipole moment remains nearly unchanged in region I [see Fig. 2]. At the extreme end of region I, some down stripes become pinched in the ST layers, yielding the formation of three-dimensional (3D) bubbles in these layers, and domain walls begin to move in the BT layers. These bubbles facilitate the first-order phase transition that occurs from regions I to II at a critical field of 2.8 MV/cm at 10 K, which results in the disappearance of the nanostripe domains and bubbles in the ST layers while the nanostripe domains still continue to exist inside the BT layers [see Fig. 1(c)]. However, the down stripes in the BT layers have a smaller width and are further apart from each other in region II than in region I, and further shrink as the magnitude of the dc field is increased in region II. The formation of a monodomain inside the ST layers (region II) makes the in-plane dipole moment relatively small while the out-of-plane dipole moment becomes large and increases with the field's magnitude (see Fig. 2). At around 3.3 MV/cm, region II transforms into region III, in which nanobubbles begin to form from the pinching of the down stripes in the BT layers while the ST layers maintain their monodomains [see Fig. 1(d)]. Interestingly, the in-plane dipole moment, originating from the ST layers, still exists at the beginning of region III but progressively disappears when further slightly increasing the dc electric field (see Fig. 2). Finally, electric fields larger than 5.1 MV/cm at 10 K lead to the vanishing of the bubbles in favor of monodomains with large polarization along the growth direction in both BT and ST layers in *region IV* [Fig. 1(e)].[25]

Interestingly, the field-induced evolution of the dipole patterns inside the BT layers in the superlattice somewhat resembles the predicted change in dipole patterns in $BaTiO_3$ *thin films* under open-circuit-like conditions and dc electric field[8] (since they both result from depolarizing field effects). However, the associated evolution of the dipole pattern inside the ST layers makes configurations depicted in Fig. 1 completely original. In particular, the overall pattern of Region II, in which periodic nanostripes in one kind of layers (BT layers, here) coexist with monodomains in the other kind of layers (ST layers, here), is an original feature. Similarly, the unusual pattern associated with Region III, in which nanobubbles form in one part of the superlattice (BT layers, here) while monodomains exist in the other part of the superlattice (ST layers, here), is original too. In other words, a dc field leads to different static characteristics of BT vs ST layers inside the same SL material. This predicted decoupling can be rationalized based on simple electrostatics. In the absence of any applied electric field, both BT and ST layers do not exhibit any depolarizing field due to the overall domain structure (the number of up dipoles is equal to the number of down dipoles). If a small applied electric field E causes one dipole to change its direction from down to up, then there is an associated energy gain $\varepsilon_g \approx -2Ep_z/V$ (where V is the unit-cell volume) due to the interaction between this dipole moment (p_z) and the electric field as well as an energy penalty of $\varepsilon_p \approx \pi p_z^2/V^2$ as a result of the creation of a depolarizing field. Consequently, such jump in direction is only possible (at low temperature) if $|\varepsilon_g| > \varepsilon_p$ or equivalently if $E > \pi p_z/2V$. Moreover, our simulations indicate that the average dipole moment in ST layers is 2.1 smaller than the corresponding one in BT layers, which

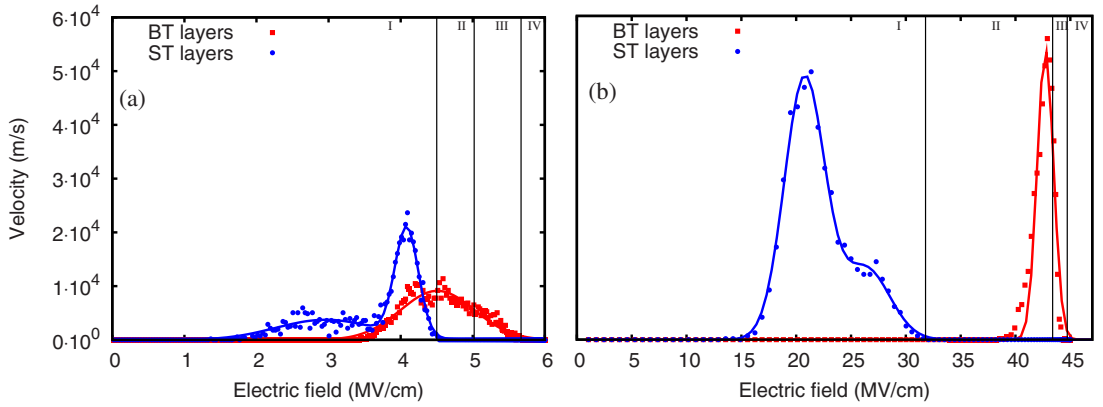

FIG. 3. (Color online) Velocities v_{BT} and v_{ST} as a function of the ac electric-field magnitude for (a) 50 GHz and (b) 2.5 THz. The solid lines represent the fit of these velocities by Eq. (2).

therefore explains why domains disappear in ST layers at much smaller fields than in BT layers.

Note that we also performed computations starting at high fields (i.e., in region IV), and then decrease the electric field until it vanishes at 10 K. We found that, in this case, the superlattice only possesses monodomain states, which are dipoles all pointing along the z direction in both BT and ST layers for fields above 2.0 MV/cm, and dipoles also pointing along an in-plane {110} direction in ST layers in addition to dipoles aligned along the [001] direction for fields below 2.0 MV/cm. The corresponding evolutions of the components of the average electric-dipole moment are shown in Fig. 2.

B. ac electric fields

Let us now focus on the *dynamics* of the domain patterns depicted in Fig. 1. For that, we apply an ac field to our superlattice, with a frequency ranging between 50 GHz (which is associated with our computational time limit) and 3.5 THz (in order to be far away from the resonant frequency that is numerically found to be around 6 THz for the studied system at 10 K). Interestingly, we found that the four regions discovered for a *static* electric field still exist for any of the investigated frequencies, provided that the amplitude of the ac field is large enough. We also numerically determined that the critical electric fields associated with the phase transition between two successive regions exponentially increase with the frequency of the applied ac field. Figures 3(a) and 3(b) display two dynamical quantities, the v_{BT} and v_{ST} velocities, for a frequency of 50 GHz and 2.5 THz, respectively, as a function of the magnitude of the ac field. Technically, $v_{BT}=A\frac{dn_{BT}}{dt}$ and $v_{ST}=A\frac{dn_{ST}}{dt}$, where A is a constant and where dn_{BT}/dt and dn_{ST}/dt represent the change in up dipoles per time in the BT and ST layers, respectively. v_{BT} quantifies the domain-wall velocity in the BT layers in regions I and II, and also provides a measure of the speed at which the dipoles flip around the ferroelectric bubbles in region III (note that v_{BT} vanishes in region IV since this latter region consists of up monodomains). Information about the speed of domain-wall and bubble motions in ST layers in *region I* are contained in v_{ST} (v_{ST} vanishes in regions II–IV). Figure 3(a) shows that, for a frequency of 50 GHz, the v_{BT}-versus-field curve is rather broad, with v_{BT} peaking around the transition from regions I to II. At high enough frequency, v_{BT} vanishes in region I and in a large part of region II while peaking close to the boundary between regions II and III [see Fig. 3(b)]. Such behaviors originate from the fact that the domain-wall motion is the predominant dynamical effect in BT layers for frequency of 50–100 GHz while, at higher frequency, dipoles flipping around the bubbles in the BT layers play bigger role. Regarding v_{ST}, Figs. 3(a) and 3(b) reveal that it exhibits *two* distinct peaks for any investigated frequency. We numerically found that the first peak (the one at smaller fields) is associated with domain-wall motions for small frequency while additional flipping of dipoles inside the down nanostripes also contributes to this first peak for larger frequency in the ST layers. The second peak is found to correspond to the dynamical evolution of the morphology and size of bubbles inside the ST layers.

Let us now discuss the general laws governing the dynamics of domain walls and bubbles in our investigated superlattices. We numerically found that neither v_{BT} nor v_{ST} follow Merz's law[26,27] for any applied field (such law has been found in bulk systems for dc field, and states that the domain-wall velocity should be proportional to $\exp(-E_a/E)$,[26,27] where E_a is the activation field and E is the applied field). Such deviation from Merz's law likely stems from the fact that nanostructures exhibit stripes with tiny periodicity (as low as a dozen of angstroms) unlike bulks for which domains are typically thousand of angstroms wide.[28] [Such suggestion is in fact confirmed by additional calculations we performed on $Pb(Zr,Ti)O_3$ ultrathin films for which we found that the domain-wall motion also deviate from Merz's law.] On the other hand, both domain-wall motions in ST and BT layers were found to obey a law previously proposed for rather small fields (that is for fields below the critical field associated with the first peak for v_{ST}, and for fields below the critical peak associated with the sole peak for v_{BT}). Such law[29] states that

$$v_{BT}(\nu) = D_{BT}(\nu)E^{4/3}\exp\left(-\frac{E_{BT,act}(\nu)}{E-E_{BT,d}}\right),$$

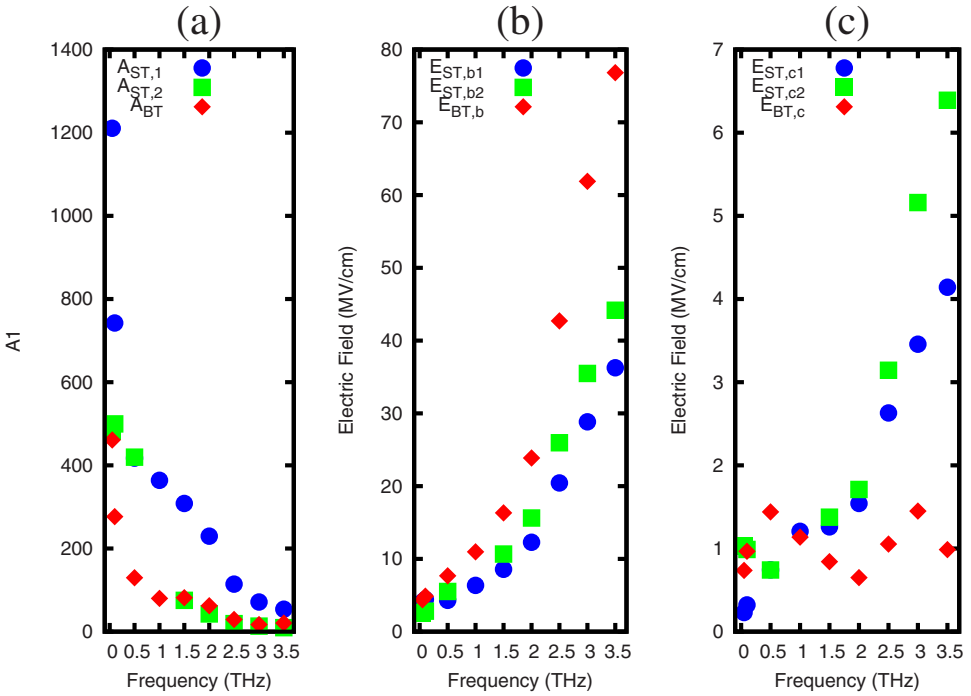

FIG. 4. (Color online) Fitting parameters of Eq. (2) as a function of frequency: (a) $A_{\mathrm{BT}}(\nu)$, $A_{\mathrm{ST},1}(\nu)$, and $A_{\mathrm{ST},2}(\nu)$; (b) $E_{\mathrm{BT},b}(\nu)$, $E_{\mathrm{ST},b1}$, and $E_{\mathrm{ST},b2}$; and (c) $E_{\mathrm{BT},c}(\nu)$, $E_{\mathrm{ST},c1}$, and $E_{\mathrm{ST},c2}$

$$v_{\mathrm{ST}}(\nu) = D_{\mathrm{ST}}(\nu)E^{4/3}\exp\left(-\frac{E_{\mathrm{ST,act}}(\nu)}{E - E_{\mathrm{ST},d}}\right), \tag{1}$$

where ν is the frequency of the applied field, and where $D_{\mathrm{BT}}(\nu)$ and $D_{\mathrm{ST}}(\nu)$ are fitting parameters. $E_{\mathrm{BT,act}}$, $E_{\mathrm{BT},d}$, $E_{\mathrm{ST,act}}$, and $E_{\mathrm{ST},d}$ all have the dimensions of electric fields.

However, Eq. (1) does not hold anymore at intermediate or high fields. In particular, they are unable to describe the dynamics of the *nanobubbles*. They also do not make $v_{\mathrm{BT}}(\nu)$ and $v_{\mathrm{ST}}(\nu)$ go to zero for very large values of the electric fields as it should be since only monodomains exist at these high fields. In fact, we numerically and *empirically* found that v_{BT} and v_{ST} can be rather well fitted for any investigated field frequency and magnitude by

$$v_{\mathrm{BT}}(\nu) = A_{\mathrm{BT}}(\nu)E^2\exp\left\{-\left[\frac{E - E_{\mathrm{BT},b}(\nu)}{E_{\mathrm{BT},c}(\nu)}\right]^2\right\},$$

$$v_{\mathrm{ST}}(\nu) = A_{\mathrm{ST},1}(\nu)E^2\exp\left\{-\left[\frac{E - E_{\mathrm{ST},b1}(\nu)}{E_{\mathrm{ST},c1}(\nu)}\right]^2\right\} + A_{\mathrm{ST},2}(\nu)E^2\exp\left\{-\left[\frac{E - E_{\mathrm{ST},b2}(\nu)}{E_{\mathrm{ST},c2}(\nu)}\right]^2\right\}, \tag{2}$$

where E is the value of the applied field, and $A_{\mathrm{BT}}(\nu)$, $A_{\mathrm{ST},1}(\nu)$, and $A_{\mathrm{ST},2}(\nu)$ all have $\mathrm{m}^3/\mathrm{V}^2$ s as SI units. $E_{\mathrm{BT},b}(\nu)$, $E_{\mathrm{BT},c}(\nu)$, $E_{\mathrm{ST},b1}$, $E_{\mathrm{ST},c1}$, $E_{\mathrm{ST},b2}$, and $E_{\mathrm{ST},c2}$ all have the dimensions of electric fields. The need for the sum of two terms in $v_{\mathrm{ST}}(\nu)$ originates from the existence of the two distinct peaks for this dynamical quantity, with the indices 1 and 2 referring to the peak associated with domain walls (and flipping of dipoles inside stripes for large frequency) and bubbles in ST layers, respectively. The evolutions of $A_{\mathrm{ST},1}(\nu)$ and $A_{\mathrm{ST},2}(\nu)$, displayed in Fig. 4(a), are such that the maximum of the first peak of v_{ST} gets closer to the maximum of its second peak as the frequency increases from 50 GHz to 1 THz, and then becomes larger than the maximum of the second peak for frequencies larger than 1.0 THz. Such tendency indicates that the bubbles become relatively slower in evolving than domain walls in moving (and individual dipoles to flip) in ST layers, as the frequency increases. Moreover, Fig. 4(b) shows that $E_{\mathrm{BT},b}(\nu)$ dramatically increases with ν, consistent with the frequency-induced shift of the peak's position of v_{BT} toward larger electric field [see Figs. 3(a) and 3(b)]. On the other hand, $E_{\mathrm{BT},c}(\nu)$ is nearly independent of the frequency [see Fig. 4(c)], reflecting the insensitivity of the width of v_{BT} with ν. Figures 4(b) and 4(c) also reveal that $E_{\mathrm{ST},b1}$, $E_{\mathrm{ST},c1}$, $E_{\mathrm{ST},b2}$, and $E_{\mathrm{ST},c2}$ all quickly increase as the frequency increases, consistent with the increased broadening and shifting toward higher fields of the two peaks of v_{ST} seen in Fig. 3, when the frequency increases.

IV. SUMMARY

In summary, first-principles-based simulations are used to determine the evolution from nanostripes to monodomains in $[BaTiO_3]_{10}/[SrTiO_3]_{10}$ superlattices under dc and ac electric fields. It is found that several different original dipole configurations can exist depending on the magnitude of the field and its frequency, including some configurations that exhibit dramatic differences in morphology between the BT and ST layers. A striking example is the coexistence of nanobubbles in BT layers with a monodomain in ST layers. Moreover, for a given value of the electric field, domain walls and nanobubbles move at a different speed inside the BT versus ST layers with these velocities deviating from the usual Merz's law.[26,27]

All these results should be qualitatively valid for BT/ST superlattices with different periods, as long as this period is long enough, since ultrashort-period superlattices do not exhibit stripe domains (but rather monodomains) for their ground states.[9] In fact, we believe that the decoupling of static and dynamical properties between different layers is a general feature of ferroelectric superlattices providing that such superlattices are made up of two (or more) materials that are sufficiently different (in terms of, e.g., their spontaneous polarization) and that the thickness of the individual layers is large enough. We thus hope that our work leads to a broad new knowledge of fundamental and technological importance in ferroelectric superlattices.

ACKNOWLEDGMENTS

This work was supported by ONR Grants No. N00014-04-1-0413 and No. N00014-08-1-0915, by NSF Grants No. DMR-0701558, No. DMR-0404335, and No. DMR-0080054 (C-SPIN), and by DOE Grant No. DE-FG02-05ER46188. Some computations were made possible thanks to the support provided by the HPCMO of the U.S. DoD, and thanks to the MRI Grant No. 0722625 from NSF.

*slisenk@uark.edu

[1] J. F. Scott, *Ferroelectric Memories*, Advanced Microelectronics Series (Springer-Verlag, Berlin, 2000).
[2] J. Scott, Science **315**, 954 (2007).
[3] M. Dawber, K. M. Rabe, and J. F. Scott, Rev. Mod. Phys. **77**, 1083 (2005).
[4] I. Ponomareva, I. Naumov, I. Kornev, H. Fu, and L. Bellaiche, Curr. Opin. Solid State Mater. Sci. **9**, 114 (2005).
[5] S. K. Streiffer, J. A. Eastman, D. D. Fong, C. Thompson, A. Munkholm, M. V. Ramana Murty, O. Auciello, G. R. Bai, and G. B. Stephenson, Phys. Rev. Lett. **89**, 067601 (2002).
[6] I. Kornev, H. Fu, and L. Bellaiche, Phys. Rev. Lett. **93**, 196104 (2004).
[7] B. K. Lai, I. Ponomareva, I. I. Naumov, I. Kornev, H. Fu, L. Bellaiche, and G. J. Salamo, Phys. Rev. Lett. **96**, 137602 (2006).
[8] B.-K. Lai, I. Ponomareva, I. A. Kornev, L. Bellaiche, and G. J. Salamo, Phys. Rev. B **75**, 085412 (2007).
[9] S. Lisenkov and L. Bellaiche, Phys. Rev. B **76**, 020102(R) (2007).
[10] A. Jiang, J. Scott, H. Lu, and Z. Chen, J. Appl. Phys. **93**, 1180 (2003).
[11] H. N. Lee, H. Christen, M. Chisholm, C. Rouleau, and D. H. Lowndes, Nature (London) **433**, 395 (2005).
[12] J. Neaton and K. Rabe, Appl. Phys. Lett. **82**, 1586 (2003).
[13] M. Dawber, N. Stucki, C. Lichtensteiger, S. Gariglio, P. Ghosez, and J.-M. Triscone, Adv. Mater. (Weinheim, Ger.) **19**, 4153 (2007).
[14] D. A. Tenne *et al.*, Science **313**, 1614 (2006).
[15] E. Bousquet, M. Dawber, N. Stucki, C. Lichtensteiger, P. Hermet, S. Gariglio, J.-M. Triscone, and P. Ghosez, Nature (London) **452**, 732 (2008).
[16] J. F. Scott and C. A. Paz de Araujo, Science **246**, 1400 (1989).
[17] V. A. Stephanovich, I. A. Luk'yanchuk, and M. G. Karkut, Phys. Rev. Lett. **94**, 047601 (2005).
[18] L. Kim, J. Kim, U. V. Waghmare, D. Jung, and J. Lee, Phys. Rev. B **72**, 214121 (2005).
[19] L. Walizer, S. Lisenkov, and L. Bellaiche, Phys. Rev. B **73**, 144105 (2006).
[20] A. García and D. Vanderbilt, in *First-Principles Calculations for Ferroelectrics*, edited by R. E. Cohen, AIP Conf. Proc. No. 436 (AIP, New York, 1998), p. 53.
[21] N. Metropolis, A. W. Rosenbluth, M. N. Rosenbluth, A. H. Teller, and E. Teller, J. Chem. Phys. **21**, 1087 (1953).
[22] I. Ponomareva, L. Bellaiche, T. Ostapchuk, J. Hlinka, and J. Petzelt, Phys. Rev. B **77**, 012102 (2008).
[23] J. Hlinka, T. Ostapchuk, D. Nuzhnyy, J. Petzelt, P. Kuzel, C. Kadlec, P. Vanek, I. Ponomareva, and L. Bellaiche, Phys. Rev. Lett. **101**, 167402 (2008).
[24] K. Johnston, X. Huang, J. B. Neaton, and K. M. Rabe, Phys. Rev. B **71**, 100103 (2005).
[25] Critical fields strongly depend on temperature. For example, at 300 K, the critical fields become equal to 0.7, 1.2, and 2.9 MV/cm for regions I to II, regions II to III, and regions III to IV transitions, respectively.
[26] W. J. Merz, Phys. Rev. **95**, 690 (1954).
[27] Y.-H. Shin, I. Grinberg, I.-W. Chen, and A. M. Rappe, Nature (London) **449**, 881 (2007).
[28] G. Catalan, A. Schilling, J. F. Scott, and J. M. Gregg, J. Phys.: Condens. Matter **19**, 132201 (2007).
[29] B. Strukov and A. Levanyuk, *Ferroelectric Phenomena in Crystals: Physical Foundations* (Springer-Verlag, New York, 1998).